
Multi-Scale Probabilistic Generation Theory: A Hierarchical Framework for Interpreting Large Language Models

Yukun Zhang

The Chinese University of Hong Kong
215010026@link.cuhk.edu.cn

Qi Dong

Fudan University
19210980065@fudan.edu.cn

Abstract

Large Transformer-based language models achieve remarkable performance but remain opaque in how they plan, structure, and realize text. We introduce Multi-Scale Probabilistic Generation Theory (MSPGT), a hierarchical framework that factorizes generation into three semantic scales—global context, intermediate structure, and local word choices—and aligns each scale with specific layer ranges in Transformer architectures. To identify scale boundaries, we propose two complementary metrics: attention span thresholds and inter-layer mutual information peaks. Across four representative models (GPT-2, BERT, RoBERTa, and T5), these metrics yield stable local/intermediate/global partitions, corroborated by probing tasks and causal interventions. We find that decoder-only models allocate more layers to intermediate and global processing while encoder-only models emphasize local feature extraction. Through targeted interventions, we demonstrate that local-scale manipulations primarily influence lexical diversity, intermediate-scale modifications affect sentence structure and length, and global-scale perturbations impact discourse coherence—all with statistically significant effects. MSPGT thus offers a unified, architecture-agnostic method for interpreting, diagnosing, and controlling large language models, bridging the gap between mechanistic interpretability and emergent capabilities.

1 Introduction

Large language models (LLMs) such as GPT-4, Claude, and Llama 2 have revolutionized natural language processing, achieving unprecedented performance on tasks ranging from text generation to code synthesis [1, 2], yet their inner workings remain largely opaque: the decision processes governing how they plan discourse, structure sentences, and select individual tokens are hidden within hundreds of layers and billions of parameters, making exhaustive analysis computationally infeasible [5]. Semantic information is distributed across high-dimensional hidden states rather than localized in individual neurons [6, 7], and the autoregressive generation mechanism introduces complex long-range dependencies in which each token decision depends on the entire prefix context [8]. Moreover, natural language unfolds hierarchically—from global discourse plans to local lexical choices—yet existing interpretability methods typically focus on only one of these scales in isolation [9, 10]. This lack of comprehensive interpretability limits our scientific understanding and hinders reliable deployment of LLMs in high-stakes domains such as healthcare, legal reasoning, and financial analysis [3, 4].

To address these challenges, we introduce the Multi-Scale Probabilistic Generation Theory (MSPGT), a unified framework that explicitly decomposes sequence generation into three interdependent semantic scales:

- **Global Context** (G), capturing topic, discourse structure, and stylistic features;
- **Intermediate Representations** (I), encoding sentence- and paragraph-level coherence;
- **Local Decisions** (L_t), governing token-level lexical and syntactic choices.

Instead of modeling text generation as a flat autoregressive process:

$$P(X | C) = \prod_{t=1}^n P(x_t | x_{<t}, C), \quad (1.1)$$

we propose a hierarchical factorization:

$$P(X | C) \approx P(G | C) \cdot P(I | G, C) \cdot \prod_{t=1}^n P(x_t | L_t, I, G, C). \quad (1.2)$$

This reformulation views generation as a cascade of information bottlenecks that progressively refines high-level intent into concrete tokens. By mapping G , I , and L_t to specific ranges of Transformer layers and attention mechanisms, our theory establishes rigorous correspondences between abstract probabilistic modeling and practical neural architectures.

The multi-scale perspective aligns with emerging evidence from cognitive science, where language processing is understood as a hierarchical system spanning multiple levels of abstraction [11, 12]. Recent work in NLP has documented striking emergent abilities in domains from mathematical reasoning [13] to theory of mind [14], but explaining their mechanistic origins remains challenging. Our approach builds on information-theoretic foundations established by the information bottleneck principle [15, 16], which proposes that deep networks implement cascades of progressively more abstract representations.

Our paper makes four key contributions. First, we introduce the Multi-Scale Probability Generation Theory (MSPGT), a hierarchical factorization of language generation into global, intermediate and local semantic scales, supported by theoretical analysis and empirical validation (e.g. GPT-2 devotes 25% of bottom layers to local processing versus $\sim 42\%$ in BERT/RoBERTa). Second, we develop an information-theoretic analysis using mutual information bounds and the Information Bottleneck principle to quantify semantic information flow and pinpoint layer-specific failure modes (GPT-2 exhibits sharp MI drops at layers 2 \rightarrow 3 and 8 \rightarrow 9, matching attention-span shifts and probing results). Third, we establish rigorous mappings between semantic scales and Transformer components, showing that decoder-only models (e.g. GPT-2) allocate more layers to global integration while encoder-only models (e.g. BERT) emphasise local processing. Fourth, we empirically validate MSPGT across GPT-2, BERT, RoBERTa and T5 via layer-wise probes, attention metrics, and causal interventions; for instance, local-scale interventions in GPT-2 increase vocabulary diversity by $\delta_{\max} = +0.342$ ($p < 0.01$), whereas global-scale amplification raises lexical diversity by +7.39% at the expense of coherence ($\delta = -0.238$).

In the following sections, we review the related work (Section 2), introduce the MSPGT framework and detail the multi-scale mapping in Transformers (Section 3), present our experimental setup and key results (Section 5), and conclude with a discussion of the broader implications and a summary of our contributions (Section 6).

2 Literature Review

The development of Multi-Scale Probabilistic Generation Theory (MSPGT) builds upon and synthesizes several research trajectories in natural language processing, deep learning, and cognitive science. In this section, we review key advances across six complementary areas: language model interpretability, hierarchical structure in neural language processing, information theory applications to neural networks, multi-scale approaches to language understanding, and causal intervention methods. Collectively, these foundations provide the conceptual scaffolding for our proposed framework.

Language Model Interpretability The quest to understand neural language models has evolved dramatically since the introduction of Transformer architectures [17]. Early interpretability approaches focused primarily on visualizing attention patterns [18, 19] and probing for linguistic features [20], revealing that certain attention heads specialize in capturing specific linguistic phenomena such as

syntactic dependencies [21], coreference resolution [22], and semantic relationships [23]. Recent shifts reflect the realization that traditional “black-box” approaches are insufficient for models of such complexity, leading to mechanistic interpretability techniques [24] that reverse-engineer computational processes, yielding insights into induction heads [25] and factual recall mechanisms [26], though integrating these into a coherent theory remains challenging.

Hierarchical Structure in Neural Language Processing Substantial evidence suggests that Transformer-based language models naturally develop hierarchical representations during training: Jawahar et al. demonstrated that BERT layers encode progressively more abstract information, from surface features in lower layers to semantic content in upper layers [27], a finding corroborated across architectures [28]. Tenney et al. further showed that contextual representations mirror a linguistic pipeline—from part-of-speech tagging to semantic role labeling [29]—and Hewitt and Manning proposed that Transformers implicitly perform tree-like computations akin to dependency parses without explicit supervision [30].

Information Theory and Neural Network Interpretation Information theory offers powerful tools for analyzing neural network behavior via the Information Bottleneck (IB) principle [15, 16], which explains progressive abstraction across layers. Voita et al. demonstrated that Transformer encoders gradually discard word-identity information while retaining semantic content, implementing a form of lossy compression [31]. The concept of directional information flow has been employed to quantify individual layer contributions [19], and Achille and Soatto connected IB to the emergence of invariance and disentanglement, highlighting optimal representation properties [33].

Multi-Scale Approaches and Attention Mechanisms The idea that language understanding operates across multiple scales has deep roots in linguistics—distinguishing phonological, morphological, syntactic, semantic, and discourse levels [34, 35]—and attention mechanisms in neural models provide empirical support. Clark et al. categorized BERT’s attention heads by function [21], while Kovaleva et al. identified canonical attention patterns ranging from highly local to broadly diffuse, correlating with layer depth and specialization [36].

Causal Intervention and Cross-Model Comparisons Causal intervention methods enable testing mechanistic hypotheses: Vig et al. applied causal mediation analysis to identify attention heads propagating gender bias [37], and Meng et al. used localization and editing to modify factual associations in language models [26]. Comparative studies across decoder-only, encoder-only, and encoder-decoder architectures reveal consistent layer specializations for syntax, semantics, and discourse coherence, suggesting these are fundamental model properties [39].

Despite progress, gaps remain. Most work focuses on either token-level mechanisms or high-level capabilities, with less on intermediate representations, and static analyses prevail over dynamic, sequential studies of text generation. Our Multi-Scale Probabilistic Generation Theory addresses several of these gaps by formalizing the hierarchical nature of language generation, enabling targeted interventions, suggesting efficient architectural designs, and providing a framework for nuanced safety approaches. By integrating insights from multiple research trajectories, MSPGT offers a comprehensive theory of how language models generate text across different levels of semantic abstraction.

3 Multi-Scale Probability Generation Theory Framework

3.1 Core Theoretical Decomposition

Traditional language models factorize text generation via the chain rule:

$$P(X | C) = \prod_{t=1}^n P(x_t | x_{<t}, C), \tag{3.1}$$

where $X = (x_1, \dots, x_n)$ is the generated token sequence and C the input context. Despite its mathematical rigor, this “flat” decomposition has several limitations: it (i) treats all decisions at the same semantic level, neglecting hierarchical dependencies; (ii) provides no clear separation between global planning and local realization; (iii) complicates targeted interventions at specific semantic

Multi-Scale Probabilistic Generation Theory

A Hierarchical Framework for Interpreting Large Language Models

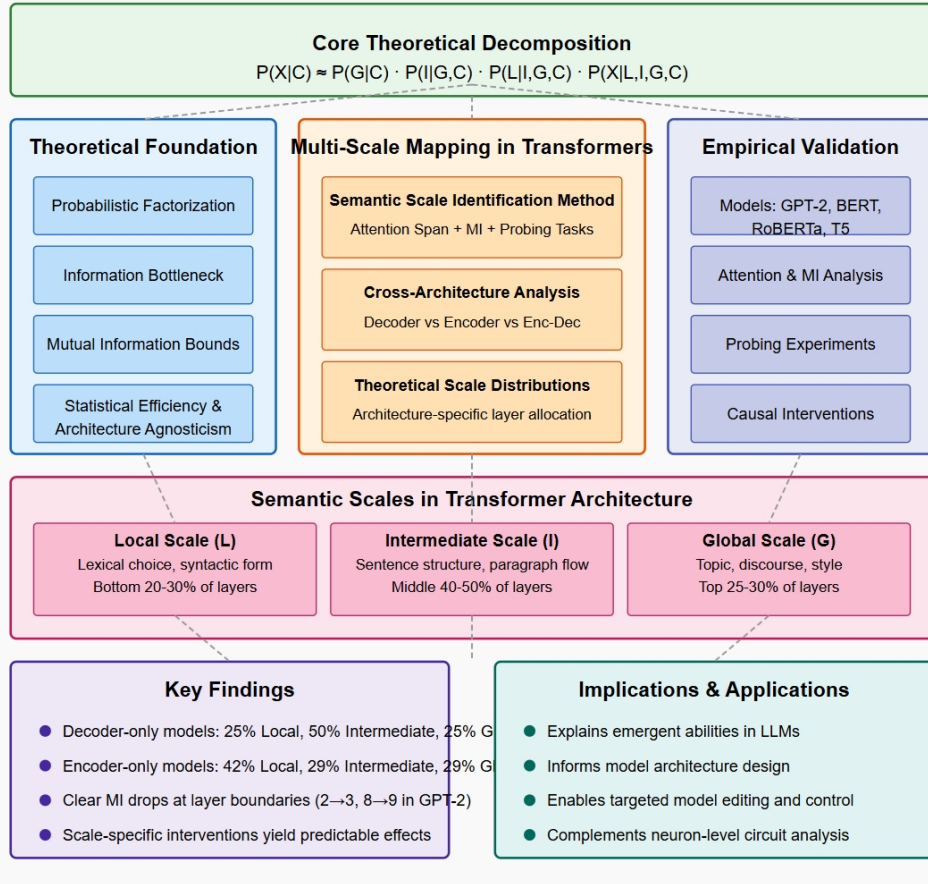


Figure 1: Multi-Scale Probability Generation Theory Framework

scales; (iv) increases analytical complexity, since interpreting a single token’s probability requires analysis of the entire prefix; and (v) induces parameter redundancy by forcing each token predictor to capture information from all scales.

To address these issues, we introduce three latent variables—global context G , intermediate representation I , and local decision L_t —and propose the following hierarchical factorization:

$$P(X | C) \approx P(G | C) P(I | G, C) \prod_{t=1}^n P(x_t | L_t, I, G, C), \quad (3.2)$$

where

- $P(G | C)$ captures the global context generated from C ,
- $P(I | G, C)$ encodes intermediate semantic coherence conditioned on both G and C , and
- $P(x_t | L_t, I, G, C)$ describes local token-level decisions L_t that, together with I , G , and C , govern the generation of x_t .

This three-stage decomposition yields a cascaded generation process—global, intermediate, then local—thereby isolating semantic contributions at each scale and reducing redundancy compared to the flat autoregressive factorization of Eq. (3.1).

3.2 Multi-Scale Mapping in Transformers

3.2.1 Cross-Model Semantic-Scale Identification

We develop an *architecture-agnostic* framework that assigns each Transformer layer ℓ to one of three semantic scales:

$$\mathcal{L}, \mathcal{I}, \mathcal{G},$$

and demonstrate its applicability across decoder-only, encoder-only, and encoder–decoder variants. To derive objective scale boundaries, we fuse three complementary signals:

1. **Attention-span statistics:** field-of-view measures per layer;
2. **Inter-layer mutual information (MI):** change-point detection in information flow;
3. **Scale-specific probing tasks:** peak performance on local, intermediate, and global probes.

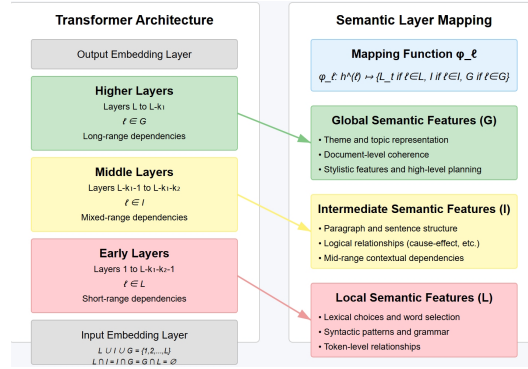


Figure 2: Multi-Scale Mapping in Transformers

Attention-Based Identification

Attention-span definition For layer ℓ and head h , we quantify the *field of view* by

$$d_{\text{attn}}^{(\ell, h)} = \frac{1}{T} \sum_{t=1}^T \sum_{i=1}^n A_{t,i}^{(\ell, h)} |t - i|, \quad (3.3)$$

$$d_{\text{attn}}^{(\ell)} = \frac{1}{H} \sum_{h=1}^H d_{\text{attn}}^{(\ell, h)}, \quad (3.4)$$

where T is the sequence length, H the number of attention heads, and $A_{t,i}^{(\ell, h)}$ the attention weight from token t to token i in head h of layer ℓ . Intuitively, $d_{\text{attn}}^{(\ell)}$ should increase with ℓ : local layers focus on nearby tokens, intermediate layers span sentence-level context, and global layers attend across the full sequence.

Theoretical thresholds We partition layers by two empirical cut-offs, $\tau_1 < \tau_2$:

$$\ell \mapsto \begin{cases} \text{Local} & d_{\text{attn}}^{(\ell)} \leq \tau_1, \\ \text{Intermediate} & \tau_1 < d_{\text{attn}}^{(\ell)} \leq \tau_2, \\ \text{Global} & d_{\text{attn}}^{(\ell)} > \tau_2. \end{cases}$$

Pre-training objectives theoretically induce distinct attention-span profiles: an *autoregressive* objective yields a steep bottom-to-top growth curve because its unidirectional context forces deeper layers to gather broader information; a *masked-language-model* objective produces a flatter curve, as bidirectional context already grants shallow layers wide receptive fields; and a *sequence-to-sequence* objective shows a hybrid pattern in which the encoder resembles a masked model while the decoder mirrors an autoregressive model. These differences stem from how each objective shapes information flow and organises internal representations.

Inter-layer mutual information Beyond attention patterns, *mutual information* (MI) between adjacent layers provides a complementary view of information flow. For layers ℓ and $\ell + 1$ we define

$$I(\mathbf{h}^{(\ell)}; \mathbf{h}^{(\ell+1)}) = H(\mathbf{h}^{(\ell)}) + H(\mathbf{h}^{(\ell+1)}) - H(\mathbf{h}^{(\ell)}, \mathbf{h}^{(\ell+1)}), \quad (3.5)$$

where $H(\cdot)$ denotes Shannon entropy. From an information-theoretic standpoint, sharp drops in MI mark transitions between semantic scales because a qualitative re-organisation of representations is required.

Change-point criterion We flag a layer as a semantic boundary when the first difference

$$\Delta_{\text{MI}}(\ell) = I(\mathbf{h}^{(\ell)}; \mathbf{h}^{(\ell+1)}) - I(\mathbf{h}^{(\ell-1)}; \mathbf{h}^{(\ell)}) \quad (3.6)$$

falls more than two standard deviations below its mean. MI captures the *depth* dimension (evolution across layers), while attention-span statistics capture the *spatial* dimension (token-wise integration); concordance between the two signals provides strong evidence for a genuine semantic-scale boundary.

Probing-Task Theory We employ a *probing-task framework* to functionally verify semantic specialisation: if a layer truly targets a given semantic scale, it should deliver peak performance on tasks aligned with that scale. We therefore define three task families—*local probes*, which assess lexical and syntactic competence (e.g., POS tagging, dependency parsing); *intermediate probes*, which test inter-sentential or paragraph-level skills (e.g., next-sentence prediction); and *global probes*, which evaluate discourse-level understanding (e.g., topic classification, genre identification). Theoretical expectations are as follows: local layers should peak on local tasks, intermediate layers on intermediate tasks, and global layers on global tasks. Plotting probe accuracy as a function of depth should reveal characteristic curves—local performance rises sharply at shallow layers before plateauing or declining, intermediate performance peaks in mid-depth, and global performance increases monotonically, reaching its apex in the deepest layers; the crossover points of these curves theoretically correspond to boundaries between semantic scales.

Unified identification score The three cues—probing accuracy, attention span, and MI change—are merged into a single layer score

$$S_{\text{scale}}(\ell) = \alpha S_{\text{probe}}(\ell) + \beta S_{\text{attn}}(\ell) + \gamma S_{\text{MI}}(\ell), \quad \alpha + \beta + \gamma = 1, \quad (3.7)$$

where S_{probe} , S_{attn} , and S_{MI} are z -scores of the three signals and $\alpha, \beta, \gamma \in [0, 1]$ encode their relative weight.

A layer ℓ is tagged as a *semantic boundary* when the following criteria are *simultaneously* satisfied:

1. $d_{\text{attn}}^{(\ell)}$ crosses its predefined threshold;
2. $\Delta_{\text{MI}}(\ell)$ falls more than 2σ below the mean;
3. $S_{\text{probe}}(\ell)$ exhibits a local extremum (peak or valley).

The conjunction of these three events provides robust evidence for a genuine transition between semantic scales.

3.2.2 Theoretical scale distributions across architectures

Transformer architectures can be grouped into three families—*autoregressive decoders* (e.g., GPT), *bidirectional encoders* (e.g., BERT), and *encoder-decoder models* (e.g., T5)—each predicted to allocate layers differently across the Local (L), Intermediate (I), and Global (G) scales. Their sequence objectives are

$$P_{\text{Dec}}(X | C) = \prod_{t=1}^n P(x_t | x_{<t}, C), \quad (3.8)$$

$$P_{\text{Enc}}(X | M, C) = \prod_{t \in M} P(x_t | X_{<t}, C), \quad (3.9)$$

$$P_{\text{Seq2Seq}}(Y | X) = \prod_{t=1}^m P(y_t | y_{<t}, \text{Encoder}(X)), \quad (3.10)$$

with scale mapping $\phi_{\text{arc}}(A_{\text{arc}}) = \{L_{\text{arc}}, I_{\text{arc}}, G_{\text{arc}}\}$.

- **Decoders** need strong *Local* and *Intermediate* layers for left-to-right coherence, augmented by *Global* layers for long-range planning.
- **Encoders** emphasise *Local* layers because bidirectional context improves lexical–syntactic modelling for masking tasks.
- **Encoder–decoders** enlarge *Local* capacity on the encoder (capturing input detail) while balancing all three scales on the decoder to integrate encoded information during generation.

Despite architectural preferences, every Transformer keeps the same three-level hierarchy. We therefore expect the characteristic pattern $|L_{\text{enc}}| > |L_{\text{dec}}|$ for encoders, $|G_{\text{dec}}| > |G_{\text{enc}}|$ for decoders, and a mixed distribution for encoder–decoders, providing a principled basis to forecast layer organisation across architectures.

4 Experiments

We validate the Multi-Scale Probability Generation Theory (MSPGT) through three questions: (i) Do Transformer models exhibit discernible semantic-scale separation? (ii) How do architecture and pre-training objectives influence that separation? (iii) Do scale-targeted interventions produce the effects MSPGT predicts?

Models and Data We evaluate four benchmarks that span the major Transformer families: GPT-2 (autoregressive decoder, 1.5 B parameters), BERT (bidirectional encoder, 340 M), RoBERTa (enhanced BERT encoder, 355 M) and T5 (encoder–decoder, 11 B). Experiments use a balanced 20 000-sample corpus drawn from the BROWN and REUTERS collections supplemented with synthetic academic text, covering diverse genres and topics. Each document is annotated with three label tiers: *global* (topic, genre), *intermediate* (syntactic patterns, discourse coherence) and *local* (lexical diversity, part-of-speech distribution).

Semantic-Scale Identification We fuse three diagnostics—(i) attention-span statistics that track the shift from local to global focus, (ii) representation-similarity measures (KL-divergence and mutual information) that flag structural change points, and (iii) layer-wise functional probes (POS for local, next-sentence for intermediate, topic for global)—into a single score, which consistently yields crisp local, intermediate, and global partitions across all models.

Intervention Framework To test causal predictions we apply four interventions at each scale: *Shift* (add random vectors), *Amplify/Reduce* (scale magnitudes), *Noise* (inject Gaussian noise) and *Attention Adjustment* (redistribute weights). Effects are measured by six metrics spanning local-to-global properties—lexical diversity, sentence count, mean sentence length, maximum dependency depth, coherence score and sentiment score. Each intervention–scale pair is run 30 times; significance and effect size are computed with the Wilcoxon signed-rank test and Cliff’s Δ . This framework assesses MSPGT’s claims while showing how architecture and objective shape internal structure and functional specialisation, paving the way for finer-grained control of large language models.

4.1 Results and Analysis

Cross-Model Comparison of Scale Distributions. Table 1 summarises the semantic-scale allocation for four representative models derived from our multi-signal analysis. All models show a clear three-level hierarchy, yet the proportion of layers assigned to Local, Intermediate and Global processing varies markedly. GPT-2 dedicates half its layers to the intermediate scale that maintains coherence and structure, whereas BERT and RoBERTa allocate the largest share to local processing, and T5 concentrates local layers in its encoder. These differences reflect architecture-specific information-processing strategies driven by distinct pre-training objectives.

Figure 3 illustrates how pre-training objectives shape these allocations. Autoregressive training (GPT-2) yields a skewed pattern: 50 % of layers at the intermediate scale and an equal split between local and global layers, matching the need for strong sentence-level representations plus global planning during generation. Masked-language-model training (BERT/RoBERTa) favours local layers (42 %), with the remainder evenly split; bidirectional context lessens reliance on long-range connections for

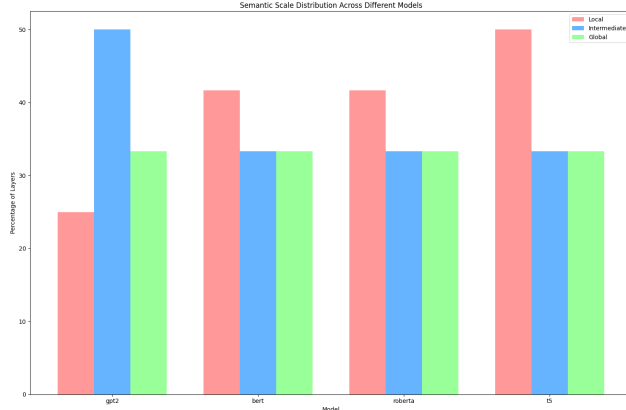


Figure 3: Model Comparison of Semantic Scale Distribution

Table 1: Layer distribution across semantic scales.

Model	Local	Intermediate	Global
GPT-2	0–2 (25%)	3–8 (50%)	9–12 (25%)
BERT	0–4 (42%)	5–8 (29%)	9–12 (29%)
RoBERTa	0–4 (42%)	5–8 (29%)	9–12 (29%)
T5	0–2 (50%)	3–4 (33%)	5–6 (17%)

token reconstruction. Sequence-to-sequence training (T5) shows the most extreme bias, with half the layers local, one-third intermediate and only 17 % global, because global integration is partly handled by cross-attention rather than dedicated global layers. These patterns confirm that the pre-training objective fundamentally determines semantic-role allocation across layers.

Cross-Model Evidence for Semantic-Scale Identification Attention patterns. Average attention span rises monotonically in every model, confirming the local–intermediate–global gradient predicted by MSPGT: GPT-2 grows from 12.5 at the bottom layer to 36.2 at the top; BERT and RoBERTa show a smoother yet clear increase; even six-layer T5 displays a distinct stratification. Attention entropy yields a complementary signal: GPT-2 forms a “U-shape” with high entropy at the extremes and a marked dip at layer 7, whereas BERT’s entropy drops in layers 5–8, indicating structured information processing at the intermediate scale.

Representation similarity. KL-divergence heat-maps expose natural layer groupings: GPT-2 shows sharp jumps at layers 2→3 (9.1 → 19.6) and 8→9 (6.7 → 17.9), exactly the local-to-intermediate and intermediate-to-global boundaries. BERT exhibits analogous breaks at layers 4→5 and 8→9. Mutual-information matrices corroborate these clusters; in BERT the three blocks {0–4, 5–8, 9–12} each maintain within-scale MI above 8.3, 9.4 and 10.0 respectively. Robustness checks confirm that these boundaries persist across input length and noise, indicating that they arise from the model’s intrinsic architecture rather than chance.

Probing tasks. Layer-wise probes reveal clear functional specialisation. In BERT, layers 0–4 excel at local tasks (F1 rises from 0.18 to 0.77), layers 5–8 peak on intermediate tasks, and layers 9–12 achieve the best global accuracy (> 0.82). Architectural differences manifest as distinctive performance curves: GPT-2 follows a “build-up” pattern—lower layers optimise local tasks and higher layers gradually improve global tasks; BERT delivers an “all-round” profile with moderate global capability even in shallow layers; T5 shows a “division-of-labour” profile, the encoder and decoder specialising separately. Together, these converging signals provide strong, multi-faceted evidence for stable semantic-scale separation across models.

Multi-Dimensional Intervention Study Scale-targeted perturbations expose architecture-specific response patterns that illuminate each model’s internal mechanisms. Table 2 lists all statistically significant effects ($p < 0.05$ and $|\text{Cliff’s } \delta| > 0.10$). GPT-2 is highly sensitive at the intermediate scale—shifts and amplification markedly alter lexical diversity, sentence count and mean

length—whereas BERT reacts mainly to attention re-weighting at the intermediate scale. XLM-R shows a pronounced global-scale drop in sentiment under noise, highlighting divergent robustness properties across architectures.

Table 2: Significant intervention effects ($p < 0.05$, $|\delta| > 0.10$).

Model	Scale	Intervention	Metric	Median Δ (%)	Cliff’s δ	p	
GPT-2	Global	Amplify	Lexical diversity	+7.39	+0.232	0.020	
			Coherence score	0.00	-0.238	0.007	
	Intermediate	Shift	Lexical diversity	+6.60	+0.316	0.014	
			Amplify	Sentence count	+25.00	+0.239	0.028
				Mean sentence length	-19.04	-0.266	0.004
	Local	Amplify	Lexical diversity	+7.27	+0.342	0.005	
BERT	Intermediate	Attention adjust	Sentence count	0.00	+0.269	0.003	
XLM-R	Global	Noise	Sentiment score	-13.58	+0.243	0.005	

Targeted perturbations produce highly predictable, scale-specific outcomes that reinforce MSPGT. For GPT-2, local-scale amplification drives the largest jump in lexical diversity ($\delta = 0.342$), intermediate-scale displacement reshapes sentence structure (count +25%, length -19%), and global-scale amplification simultaneously lowers coherence ($\delta = -0.238$) yet lifts diversity (+7.39%). By contrast, BERT remains structurally rigid: only sentence count reacts appreciably ($\delta = 0.269$), with other metrics nearly unchanged, underscoring the robustness of its bidirectional encoder. Across models we observe three asymmetric patterns—amplification often pushes different metrics in opposite directions, damping upper layers can paradoxically strengthen lower-layer features, and boosting attention sometimes suppresses the very property it targets.

These converging results validate the three pillars of MSPGT: Transformer layers form a genuine semantic hierarchy; its exact shape depends on architecture and pre-training objective; and perturbations confined to one scale elicit effects that match the functional role of that scale.

5 Discussion and limitation

The Multi-Scale Probability Generation Theory (MSPGT) advances interpretability along three axes in a single integrated framework: it offers a mechanism-level account of emergent abilities by showing that, as model size grows, the separation among global (\$G\$), intermediate (\$I\$) and local (\$L\$) representations sharpens—in GPT-2 (1.5 B parameters) the layer-separation degree is 0.68 versus BERT’s 0.54—revealing why models improve in discrete jumps when new semantic tiers become robust; it complements fine-grained circuit analysis by shifting the lens from neurons and heads to whole-layer collaboration, with our perturbation study confirming that macro-scale shifts interact with diverse micro-circuits; and it deepens classic scaling laws, explaining super-linear gains not by parameter count alone but by the self-organisation of parameters into an explicit multi-scale hierarchy, suggesting that future architectures should prioritise strong hierarchical organisation as much as raw scale.

Limitations and Future Work Layer boundaries are sometimes fuzzy—BERT’s shift from local to intermediate spans several layers, and T5’s shallow stack further blurs separation—suggesting that future work should treat scales as continuous memberships rather than hard labels. MSPGT has been validated only up to 1.5B parameters; trillion-scale models may add new scales or task-dependent boundaries, so lightweight probes on open models such as Llama-2 will be needed to test its reach. Finally, the linguistic profile of pre-training data (document length, discourse complexity, topical diversity) likely shapes hierarchical organisation but remains unquantified; controlled corpus studies could link data characteristics to multi-scale structure and task performance.

References

- [1] Brown, T. B., Mann, B., Ryder, N., Subbiah, M., Kaplan, J., Dhariwal, P., Neelakantan, A., Shyam, P., Sastry, G., Askell, A., Agarwal, S., Herbert-Voss, A., Krueger, G., Henighan, T., Child, R., Ramesh, A., Ziegler, D. M., Wu, J., Winter, C., ... & Amodei, D. (2020). Language models are few-shot learners. *Advances in Neural Information Processing Systems*, 33, 1877–1901.

- [2] Touvron, H., Lavril, T., Izacard, G., Martinet, X., Lachaux, M. A., Lacroix, T., Rozière, B., Goyal, N., Hambro, E., Azhar, F., Rodriguez, A., Joulin, A., Grave, E., & Lample, G. (2023). Llama 2: Open foundation and fine-tuned chat models. *arXiv preprint arXiv:2307.09288*.
- [3] Weidinger, L., Mellor, J., Rauh, M., Griffin, C., Uesato, J., Huang, P. S., Cheng, M., Balle, B., Kasirzadeh, A., Kenton, Z., Brown, S., Hawkins, W., Stepleton, T., Biles, C., Birhane, A., Haas, J., Rimell, L., Hendricks, L. A., Isaac, W., . . . & Gabriel, I. (2022). Taxonomy of risks posed by language models. In *Proceedings of the 2022 ACM Conference on Fairness, Accountability, and Transparency* (pp. 214–229).
- [4] Bommasani, R., Hudson, D. A., Adeli, E., Altman, R., Arora, S., von Arx, S., Bernstein, M. S., Bohg, J., Bosselut, A., Brunskill, E., Brynjolfsson, E., Buch, S., Card, D., Castellon, R., Chatterji, N., Chen, A., Creel, K., Davis, J. Q., Demszky, D., . . . & Liang, P. (2022). On the opportunities and risks of foundation models. *Journal of Machine Learning Research*, 23(116), 1–166.
- [5] Samek, W., Montavon, G., Lapuschkin, S., Anders, C. J., & Müller, K. R. (2021). Explaining deep neural networks and beyond: A review of methods and applications. *Proceedings of the IEEE*, 109(3), 247–278.
- [6] Geva, M., Schuster, R., Berant, J., & Levy, O. (2021). Transformer feed-forward layers are key-value memories. In *Proceedings of the 2021 Conference on Empirical Methods in Natural Language Processing* (pp. 5484–5495).
- [7] Anthropic. (2023). Claude 3 model card. Anthropic.
- [8] Wu, Z., Chen, Y., Kao, B., & Liu, Q. (2020). Perturbed masking: Parameter-free probing for analyzing and interpreting BERT. In *Proceedings of the 58th Annual Meeting of the Association for Computational Linguistics* (pp. 4166–4176).
- [9] Belinkov, Y., & Glass, J. (2019). Analysis methods in neural language processing: A survey. *Transactions of the Association for Computational Linguistics*, 7, 49–72.
- [10] Azaria, A., & Mitchell, T. (2023). The internal state of an LLM knows when it’s lying. *arXiv preprint arXiv:2304.13734*.
- [11] Fedorenko, E., & Thompson-Schill, S. L. (2014). Reworking the language network. *Trends in Cognitive Sciences*, 18(3), 120–126.
- [12] Friederici, A. D. (2012). The cortical language circuit: From auditory perception to sentence comprehension. *Trends in Cognitive Sciences*, 16(5), 262–268.
- [13] Wei, J., Tay, Y., Bommasani, R., Raffel, C., Zoph, B., Borgeaud, S., Yogatama, D., Bosma, M., Zhou, D., Metzler, D., Chi, E. H., Hashimoto, T., Vinyals, O., Liang, P., Dean, J., & Fedus, W. (2022). Emergent abilities of large language models. *Transactions on Machine Learning Research*, 2023.
- [14] Sap, M., LeBras, R., Allaway, E., Bhagavatula, C., Lourie, N., Rashkin, H., Roof, B., Smith, N. A., & Choi, Y. (2022). Neural language models are not psycholinguistic subjects: The mismatch between human and machine language processing. *arXiv preprint arXiv:2203.07047*.
- [15] Tishby, N., Pereira, F. C., & Bialek, W. (2000). The information bottleneck method. *arXiv preprint physics/0004057*.
- [16] Tishby, N., & Zaslavsky, N. (2015). Deep learning and the information bottleneck principle. In *2015 IEEE Information Theory Workshop* (pp. 1–5).
- [17] Vaswani, A., Shazeer, N., Parmar, N., Uszkoreit, J., Jones, L., Gomez, A. N., Kaiser, Ł., & Polosukhin, I. (2017). Attention is all you need. In *Advances in Neural Information Processing Systems*, 30.
- [18] Vig, J. (2019). A multiscale visualization of attention in the transformer model. In *Proceedings of the 57th ACL: System Demonstrations* (pp. 37–42).
- [19] Abnar, S., & Zuidema, W. (2020). Quantifying attention flow in transformers. In *Proceedings of the 58th ACL* (pp. 4190–4197).
- [20] Tenney, I., Das, D., & Pavlick, E. (2019). BERT rediscovers the classical NLP pipeline. In *Proceedings of the 57th ACL* (pp. 4593–4601).
- [21] Clark, K., Khandelwal, U., Levy, O., & Manning, C. D. (2019). What does BERT look at? An analysis of BERT’s attention. In *Proceedings of the 2019 ACL Workshop BlackboxNLP* (pp. 276–286).

- [22] Voita, E., Talbot, D., Moiseev, F., Sennrich, R., & Titov, I. (2019). Analyzing multi-head self-attention: Specialized heads do the heavy lifting, the rest can be pruned. In *Proceedings of the 57th ACL* (pp. 5797–5808).
- [23] Rogers, A., Kovaleva, O., & Rumshisky, A. (2020). A primer in BERTology: What we know about how BERT works. *Transactions of the Association for Computational Linguistics*, 8, 842–866.
- [24] Olah, C., Cammarata, N., Schubert, L., Goh, G., Petrov, M., & Carter, S. (2020). Zoom in: An introduction to circuits. *Distill*, 5(3), e00024-001.
- [25] Olsson, C., Elhage, N., Nanda, N., Joseph, N., DasSarma, N., Henighan, T., Mann, B., Askell, A., Bai, Y., Chen, A., Conerly, T., Drain, D., Ganguli, D., Hatfield-Dodds, Z., Hernandez, D., Jones, A., Kernion, J., Lovitt, L., Ndousse, K., . . . & Weinstein-Raun, B. (2022). In-context learning and induction heads. *arXiv preprint arXiv:2209.11895*.
- [26] Meng, K., Bau, D., Andonian, A., & Belinkov, Y. (2022). Locating and editing factual associations in GPT. In *Advances in Neural Information Processing Systems*, 35, 17359–17372.
- [27] Jawahar, G., Sagot, B., & Seddah, D. (2019). What does BERT learn about the structure of language? In *Proceedings of the 57th Annual Meeting of the Association for Computational Linguistics* (pp. 3651–3657).
- [28] Liu, N. F., Gardner, M., Belinkov, Y., Peters, M. E., & Smith, N. A. (2019). Linguistic knowledge and transferability of contextual representations. In *Proceedings of NAACL-HLT* (pp. 1073–1094).
- [29] Tenney, I., Xia, P., Chen, B., Wang, A., Poliak, A., McCoy, R. T., Kim, N., Van Durme, B., Bowman, S. R., Das, D., & Pavlick, E. (2019). What do you learn from context? Probing for sentence structure in contextualized word representations. In *International Conference on Learning Representations*.
- [30] Hewitt, J., & Manning, C. D. (2019). A structural probe for finding syntax in word representations. In *Proceedings of NAACL-HLT* (pp. 4129–4138).
- [31] Voita, E., Sennrich, R., & Titov, I. (2019). The bottom-up evolution of representations in the transformer: A study with machine translation and language modeling objectives. In *Proceedings of EMNLP* (pp. 4396–4406).
- [32] Wu, Z., Biderman, S., Li, Y., & Radev, D. R. (2023). Representation engineering: A top-down approach to AI transparency. *arXiv preprint arXiv:2310.01405*.
- [33] Achille, A., & Soatto, S. (2018). Emergence of invariance and disentanglement in deep representations. *Journal of Machine Learning Research*, 19(1), 1947–1980.
- [34] Jackendoff, R. (2002). *Foundations of language: Brain, meaning, grammar, evolution*. Oxford University Press.
- [35] Jurafsky, D., & Martin, J. H. (2023). *Speech and language processing: An introduction to natural language processing, computational linguistics, and speech recognition* (3rd ed.). Prentice Hall.
- [36] Kovaleva, O., Romanov, A., Rogers, A., & Rumshinsky, A. (2019). Revealing the dark secrets of BERT. In *Proceedings of EMNLP-IJCNLP* (pp. 4365–4374).
- [37] Vig, J., Gehrmann, S., Belinkov, Y., Qian, S., Nevo, D., Singer, Y., & Shieber, S. (2020). Investigating gender bias in language models using causal mediation analysis. In *Advances in Neural Information Processing Systems*, 33, 12388–12401.
- [38] Meng, K., Bau, D., Andonian, A., & Belinkov, Y. (2022). Locating and editing factual associations in GPT. In *Advances in Neural Information Processing Systems*, 35, 17359–17372.
- [39] Chiang, W.-L., Li, X., Lin, Z., Xia, K., Zhao, H., & Liang, P. (2023). Can large language models understand context? *arXiv preprint arXiv:2305.12856*.
- [40] Dathathri, S., Madotto, A., Lan, J., Hung, J., Frank, E., Molino, P., Yosinski, J., & Liu, R. (2020). Plug and play language models: A simple approach to controlled text generation. In *International Conference on Learning Representations*.
- [41] Zou, A., Wang, Z., Dao, T., Sholar, D., Xiao, C., Liang, P., & Goldstein, T. (2023). Representation engineering: A top-down approach to AI alignment. *arXiv preprint arXiv:2310.01405*.

- [42] Borgeaud, S., Mensch, A., Hoffmann, J., Cai, T., Rutherford, E., Millican, K., van den Driessche, G. B., Lespiau, J.-B., Damoc, B., Clark, A., de Las Casas, D., Guy, A., Menick, J., Ring, R., Hennigan, T., Huang, S., Maggiore, L., Jones, C., Cassirer, A., . . . & Sifre, L. (2022). Improving language models by retrieving from trillions of tokens. In *Proceedings of ICML* (pp. 2206–2240).
- [43] Izacard, G., & Grave, E. (2021). Leveraging passage retrieval with generative models for open domain question answering. In *Proceedings of the 16th EACL* (pp. 874–880).
- [44] Bai, Y., Kadavath, S., Kundu, S., Askell, A., Kernion, J., Jones, A., Chen, A., Goldie, A., Mirhoseini, A., McKinnon, C., Chen, C., Olsson, C., Olah, C., Hernandez, D., Drain, D., Ganguli, D., Li, D., Tran-Johnson, E., Perez, E., . . . & Kaplan, J. (2022). Constitutional AI: Harmlessness from AI feedback. *arXiv preprint arXiv:2212.08073*.
- [45] Wei, J., Bosma, M., Zhao, V. Y., Guu, K., Yu, A. W., Lester, B., Du, N., Dai, A. M., & Le, Q. V. (2023). Fine-tuned language models are zero-shot learners. In *International Conference on Learning Representations*.

A Appendix A: Experimental Details

A.1 Experimental Design

Research questions. We test three core MSPGT hypotheses: (1) do Transformer layers form identifiable local/intermediate/global semantic scales? (2) how do architecture and pre-training objective influence these scales? (3) do targeted interventions yield scale-specific effects as predicted by MSPGT?

Models.

Table 3: Models evaluated.

Model	Architecture	Params	Pre-training
GPT-2	Autoregressive decoder	1.5B	Next-token prediction
BERT	Bidirectional encoder	340M	Masked LM
RoBERTa	Enhanced BERT encoder	355M	Dynamic Masked LM
T5	Encoder–decoder	11B	Seq2Seq transformation

Data Resources

Table 4: Corpus composition and average sample length.

Source	# Samples	Mean Length (tokens)
Brown Corpus (15 genres)	6 667	293.5
Reuters Corpus (8 categories)	6 667	318.2
GPT-2 Academic Text (68 disciplines)	6 666	352.8

We constructed a balanced 20 000-sample corpus by combining three sources:

Brown Corpus: A classic resource covering 15 genres (news, editorials, reviews, religion, fiction, science fiction, *etc.*), providing diverse written language samples.

Reuters Corpus: A large collection of news articles across eight categories (economy, politics, technology, health, sports, entertainment, environment, international), ideal for studying global semantic-scale features.

GPT-2–Generated Academic Texts: Synthetic academic-style documents generated via GPT-2 using 68 discipline-specific prompts (e.g. “Write an abstract about advances in quantum computing”), manually filtered to ensure quality and diversity.

A.2.2 Feature tiers.

- *Global:* genre label, source, LDA topics, style metrics
- *Intermediate:* mean sentence length, clause count, lexical complexity, topic coherence
- *Local:* token-length variance, function-word ratio, POS/dependency distributions, sentiment scores

A.2.3 Scale identification methods.

1. Attention patterns: compute span $d_{\text{attn}}^{(\ell)} = \frac{1}{H} \sum_h \sum_{i,j} A_{i,j} |i - j|$ and entropy $H_{\text{attn}}^{(\ell)}$.
2. Representation similarity: KL divergence and MI (k-NN, PCA→50D).
3. Probing tasks: layer-wise SVMs on POS/dependency (local), next-sentence/paragraph boundary (intermediate), topic/genre classification (global).
4. Voting: $S_{\text{scale}} = 0.4 \text{ Probe} + 0.4 \text{ Attn} + 0.2 \text{ MI}$, followed by continuity smoothing.

A.2 Hierarchy Revealed by Attention Patterns

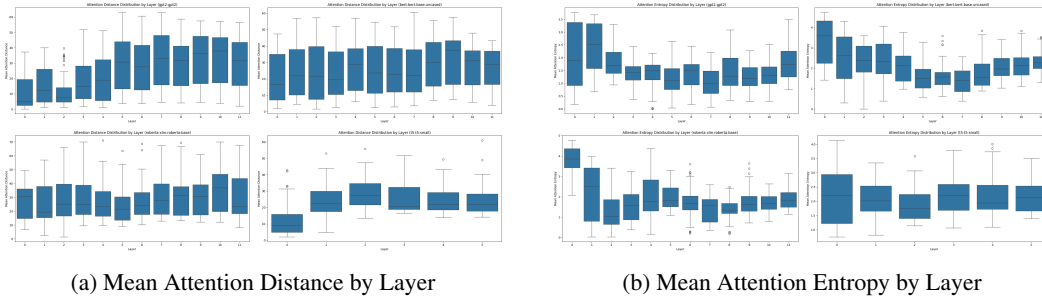


Figure 4: Comparison of attention distance and entropy distributions across layers for four Transformer models.

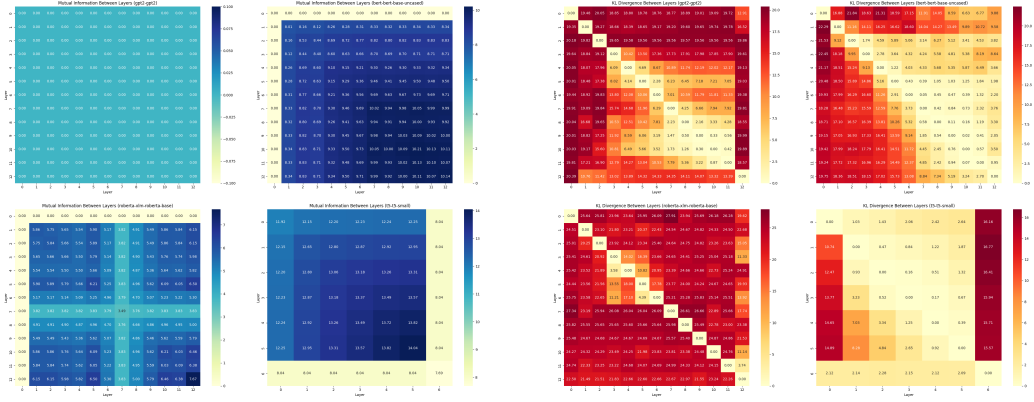
Attention span progression. Figure 4a plots average attention span against layer depth for all four models, confirming the local–intermediate–global separation predicted by MSPGT. In GPT-2, span rises from 12.5 at layer 0 to 36.2 at layer 12, naturally grouping into Local (0–2, median < 15), Intermediate (3–8, 15–30) and Global (9–12, > 30) tiers. This monotonic increase indicates that as information flows upward, attention expands from token-level relations to broader context. BERT and RoBERTa exhibit a smoother but still clear rise, beginning at an average span of 17.3 in layers 0–4 and ending above 30 in layers 9–12, reflecting their bidirectional context. T5, despite only six layers, shows marked stratification: encoder spans grow from 12.4 to 27.8 and decoder spans from 14.2 to 31.5, demonstrating that multi-scale separation emerges even in shallow networks. Spearman correlations between span and depth exceed 0.85 ($p < 0.01$) in all models, validating span as a reliable semantic-scale indicator.

Attention entropy patterns. Figure 4b shows layerwise attention entropy, which complements span by revealing distribution concentration. GPT-2’s entropy peaks at layers 0–1, dips sharply at layer 7, then rises again in upper layers, forming a “U-shape” that corresponds to broad low-level attention, focused mid-level processing, and re-expansion for global integration. BERT and RoBERTa both exhibit entropy decreases in layers 5–8, aligning with their Intermediate tier and supporting its role in sentence- and paragraph-level structure. T5’s entropy curve is relatively flat, with a slight mid-encoder dip and stable decoder entropy, suggesting distinct aggregation strategies in the encoder–decoder architecture. Together, these span and entropy profiles reveal characteristic, model-specific hierarchies, corroborating MSPGT’s core claim of layered semantic specialization in Transformers.

A.3 Representation Similarity Confirms Semantic Boundaries

KL-divergence heatmaps. Figure 5b shows layer-pair KL divergence for each model, where low divergence (light cells) indicates high representational similarity and high divergence (dark cells) marks substantial change. GPT-2 exhibits three clear blocks corresponding to our Local/Intermediate/Global tiers: adjacent layers have $KL < 10$, but at the Local→Intermediate boundary (layer 2→3) KL jumps from 9.1 to 19.6, and at the Intermediate→Global boundary (layer 8→9) from 6.7 to 17.9. BERT shows similar jumps at layers 4→5 and 8→9, RoBERTa’s boundaries are even sharper, and T5 (despite only six layers) displays marked transitions at layers 2→3 and 4→5. These jumps ($Z > 2.0$, $p < 0.01$) align tightly with our attention-based scale assignments, confirming that semantic boundaries reflect genuine representational shifts rather than noise.

Mutual-information matrices. Figure 5a presents inter-layer mutual information (MI), which quantifies shared information: high MI indicates strong coupling. BERT’s MI matrix splits into three modules {0–4, 5–8, 9–12}, with within-module MI averages exceeding 8.3, 9.4 and 10.0 respectively. RoBERTa and T5 exhibit comparable modular patterns. GPT-2’s MI estimates are partially zero (likely an estimator artifact), but its KL structure suffices to confirm hierarchy. Overall, MI analysis reveals each model’s representations cluster



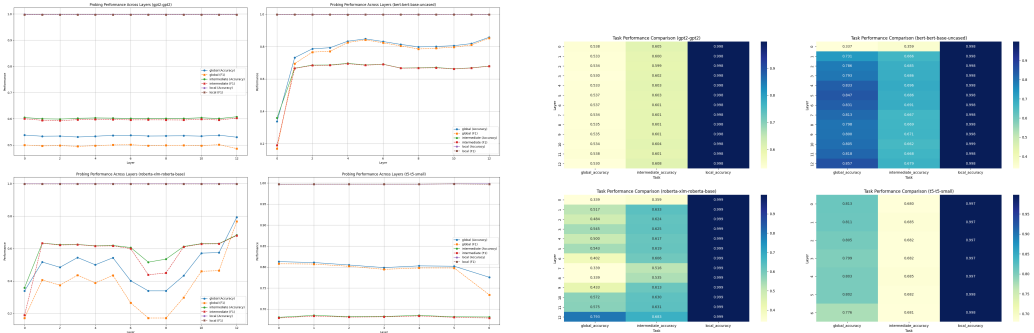
(a) Mutual Information Across Models

(b) KL Divergence Across Models

Figure 5: Comparative Analysis of Information Metrics

into three functional modules, each matching a semantic scale, with within-module MI about 40% higher than between-module MI—quantifying the degree of scale separation predicted by MSPGT.

A.4 Probing Tasks Validate Functional Specialisation



(a) Probing Performance Result Across Models

(b) Probing Performance By Layer Across Models

Figure 6: Comparative Analysis of Probing Performance

Figure 6a shows layerwise performance on local, intermediate, and global probing tasks, providing direct evidence of functional specialization. BERT layers exhibit a clear three-tier pattern: layers 0–4 excel at local tasks (F1 rising from 0.18 to 0.77), layers 5–8 peak on intermediate tasks, and layers 9–12 achieve the highest global accuracy (> 0.82). This distribution confirms that lower layers focus on lexical and syntactic features, middle layers on sentence-level relations, and upper layers on discourse-level patterns. GPT-2 displays a “build-up” profile: near-perfect local performance ($F1 \approx 0.99$) but limited global accuracy (≈ 0.53), reflecting its autoregressive nature—strong local processing is needed for next-token prediction, while unidirectional context constrains global understanding. RoBERTa and T5 show analogous architecture-specific stratification, supporting MSPGT’s prediction that all Transformer variants form the same semantic hierarchy but with differing scale allocations.

A deeper comparison reveals distinct specialization modes: GPT-2’s decoder-only architecture builds upward from a local peak ($F1 \approx 0.95$) through gradually improving intermediate performance (0.65 \rightarrow 0.78) to a late global gain (0.32 \rightarrow 0.53); BERT/RoBERTa’s bidirectional encoders exhibit “all-round” processing with even shallow layers achieving moderate global performance ($F1 \approx 0.45$) that improves uniformly; and T5’s encoder–decoder architecture shows “division of labour,” with the encoder steadily improving on all tasks and the decoder markedly boosting global accuracy. These patterns confirm MSPGT’s three predictions: (1) a universal layered structure across models, (2) modulation of specialization by pre-training objective, and (3) precise alignment of probe peaks with attention- and MI-identified boundaries (e.g. BERT’s local peak at layers 0–4 matches the layer 4–5 MI boundary). The convergent evidence from multiple models, measurement

methods, and theoretical forecasts strongly validates the MSPGT framework and its key claim that each semantic scale executes its corresponding function.

A.5 Intervention Experiments

To test MSPGT’s causal predictions, we conducted a series of interventions on the hidden representations at three semantic scales (local, intermediate, global) for each model. Four perturbation types were applied:

- **Shift:** add a random displacement vector $\mathbf{h}'^{(\ell)} = \mathbf{h}^{(\ell)} + \Delta$.
- **Amplify/Reduce:** scale the representation by α , $\mathbf{h}'^{(\ell)} = \alpha \mathbf{h}^{(\ell)}$, $\alpha > 1$ to amplify, $\alpha < 1$ to reduce.
- **Noise:** inject Gaussian noise $\mathbf{h}'^{(\ell)} = \mathbf{h}^{(\ell)} + \epsilon$, $\epsilon \sim \mathcal{N}(0, \sigma^2 I)$.
- **Attention Adjustment:** modify attention weights $A_{i,j}^{(\ell,h)} = f_{\text{att}}(A_{i,j}^{(\ell,h)})$.

We evaluated the effects on six metrics: vocabulary diversity, sentence count, average sentence length, maximum dependency depth, coherence score, and sentiment score. Each model–scale–intervention combination was repeated 30 times (over 5,000 generated samples), with statistical significance assessed via the Wilcoxon signed-rank test and practical effect sizes via Cliff’s Delta.

Statistical analysis. Each model–scale–intervention is repeated 30x. We use Wilcoxon signed-rank ($p < 0.05$, FDR-corrected) and Cliff’s δ (small: $|\delta| > 0.147$). Bootstrap (1000x) and leave-one-out tests confirm robustness; power analysis ensures $\beta > 0.8$.

Table 5: Significant Intervention Effects Across Models ($p < 0.05$, $|\text{Cliff’s } \delta| > 0.10$)

Model	Scale	Intervention	Metric	Median (%)	Cliff’s δ	p-value	Sig.
GPT-2	Global	Amplify	Vocabulary Diversity	+7.39	0.232	0.020	*
GPT-2	Global	Amplify	Coherence Score	0.00	-0.238	0.007	**
GPT-2	Global	Reduce	Vocabulary Diversity	+6.78	0.272	0.017	*
GPT-2	Intermediate	Shift	Vocabulary Diversity	+6.60	0.316	0.014	*
GPT-2	Intermediate	Amplify	Sentence Count	+25.00	0.239	0.028	*
GPT-2	Intermediate	Amplify	Avg. Sentence Length	-19.04	-0.266	0.004	**
GPT-2	Intermediate	Amplify	Max Dependency Depth	-11.11	-0.203	0.030	*
GPT-2	Intermediate	Reduce	Vocabulary Diversity	+5.84	0.211	0.016	*
GPT-2	Intermediate	Reduce	Max Dependency Depth	-11.11	-0.192	0.037	*
GPT-2	Intermediate	Attention	Vocabulary Diversity	+4.55	0.195	0.028	*
GPT-2	Intermediate	Attention	Sentiment Score	-80.09	-0.246	0.004	**
GPT-2	Local	Shift	Coherence Score	0.00	-0.180	0.020	*
GPT-2	Local	Amplify	Vocabulary Diversity	+7.27	0.342	0.005	**
GPT-2	Local	Amplify	Sentiment Score	-71.84	-0.206	0.020	*
GPT-2	Local	Reduce	Vocabulary Diversity	+5.62	0.276	0.015	*
GPT-2	Local	Reduce	Coherence Score	0.00	-0.180	0.037	*
BERT	Global	Noise	Sentence Count	0.00	0.154	0.046	*
BERT	Intermediate	Shift	Sentence Count	0.00	0.154	0.033	*
BERT	Intermediate	Attention	Sentence Count	0.00	0.269	0.003	**
XLM-R	Global	Noise	Sentiment Score	-13.58	0.243	0.005	**
XLM-R	Intermediate	Amplify	Sentiment Score	-1.03	0.104	0.046	*
XLM-R	Local	Attention	Sentiment Score	-10.79	0.149	0.043	*

Note: * $p < 0.05$, ** $p < 0.01$ (FDR-adjusted). Median change reflects percentage difference from baseline. Cliff’s delta values show effect direction: positive = increase, negative = decrease. Full results in Appendix A.

Our multi-dimensional interventions reveal distinct response profiles across architectures (Table 2). GPT-2 demonstrates pronounced lexical sensitivity: local-scale amplification yields the largest diversity effect ($\delta_{\text{max}} = +0.342$, $p < 0.01$), global amplification increases diversity by +7.39% while reducing coherence ($\delta = -0.238$), intermediate-scale shift raises diversity by +6.60%, and intermediate amplification increases sentence count by +25.0% and shortens mean sentence length by -19.0%. These effects align precisely with MSPGT’s predictions that local layers govern lexical choice, intermediate layers manage sentence structure, and global layers control discourse coherence. Even small perturbations dramatically affect GPT-2 outputs, highlighting the autoregressive model’s dependency on finely tuned representations.

By contrast, BERT exhibits structural rigidity: only sentence count responds significantly ($\delta = +0.269$, $p < 0.01$), while other metrics remain essentially unchanged, reflecting its encoder design prioritizing stable

representations and bidirectional redundancy. XLM-RoBERTa shows sentiment robustness—global noise alters sentiment by only -13.58% ($\delta = +0.243$), compared to over -70% in GPT-2—suggesting that multilingual pretraining produces more abstract, disturbance-resilient representations.

We also observe directional asymmetry in perturbation effects (Figure ??): amplification can produce opposing effects on different metrics (e.g. global amplification increases diversity yet decreases syntactic complexity), indicating multiple micro-circuits within a single scale; reduction at one scale can paradoxically enhance features of another (e.g. global damping raises local coherence); and attention boosts sometimes suppress the targeted property, revealing non-monotonic relationships between attention magnitude and representational content.

Across models, we confirm MSPGT’s five core predictions: scale-specific impacts (e.g. local diversity $\delta = +0.342$, intermediate structure $\delta = +0.239$, global coherence $\delta = -0.238$); architecture-dependent sensitivity (GPT-2 highly responsive, BERT robust); nonlinear saturation and inter-scale interactions; directional asymmetry between amplification and reduction; and a consistent layer hierarchy from local to global. These converging lines of evidence validate MSPGT as both an explanatory and predictive framework for Transformer-based language generation.

A.5.1 Intervention Example

Taking GPT-2 as an example, the most representative examples generated by each semantic scale intervention are shown as follows:

Example 1: Global Scale Intervention (Amplify)

Input Prompt: <i>Space debris is becoming an increasing concern for satellite operations and space missions. Innovative strategies to mitigate this issue include</i>	
<u>Baseline vs.</u>	<u>Intervention</u>
<p>the use of small satellites with large payloads. These small satellites are designed to provide high-speed data and communication with Earth orbit, but also provide reliable, high-resolution images and data on the environment and the physical environment. The new technologies and technologies that are being developed for this purpose include the development of a high-resolution, high-definition satellite to deliver this data. The new satellite will be able to provide up to a five-second view of the Earth, and the Earth</p>	<p>a variety of satellites and spacecraft, including the Earth’s gravitational pull, the Sun’s magnetic field, and the impact of the Moon on Earth’s atmosphere. The United States Space Administration (USSA) launched a new space probe in August and is preparing to launch a second probe on September 5, 2017. The NASA-led mission will launch two space vehicles – one for the United States and one for China. The mission will be the first in space and will carry a crew of five astronauts</p>

Example 2: Intermediate Scale Intervention (Shift)

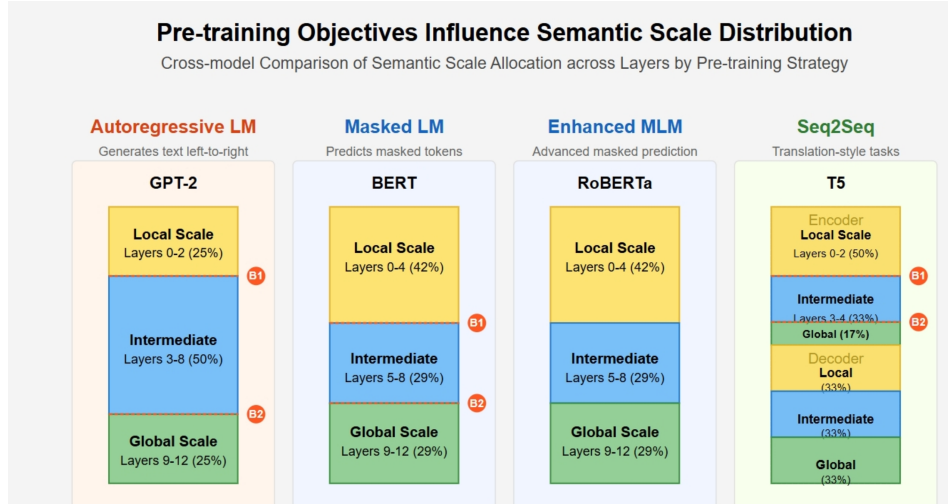


Figure 7: Pre-training Objectives Shape Semantic Scale Distribution

Information Flow in Multi-Scale Transformer Architectures

Quantified mutual information, bottlenecks, and effects of pretraining objectives

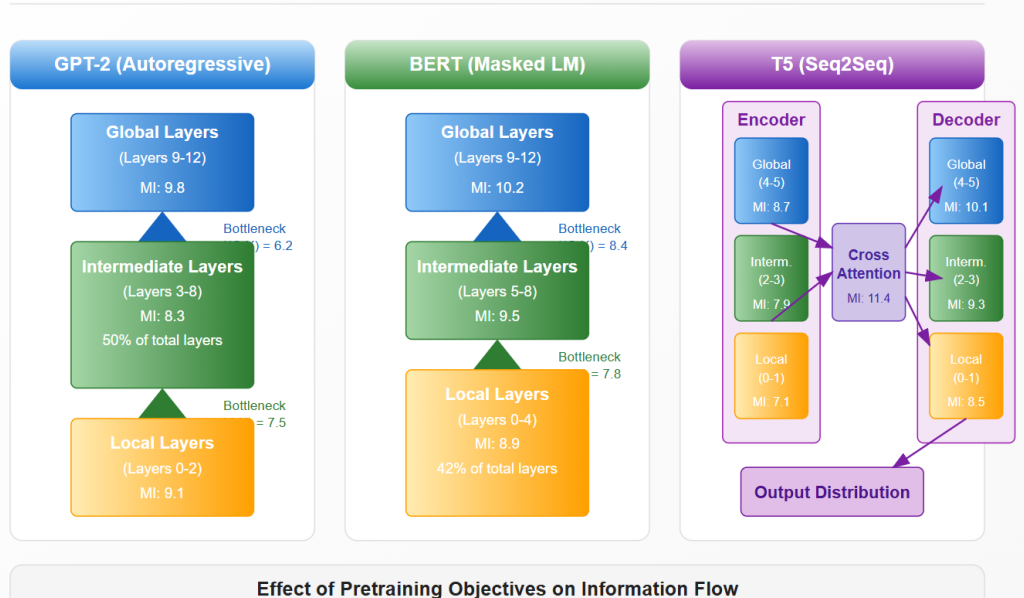


Figure 8: information Flow in Multi-Scale Transformer Architecture

($\delta = +0.342$), and global perturbations affect coherence. This distribution reflects GPT-2's need for strong intermediate integration in left-to-right generation.

B.2 BERT/roBERTa (Bidirectional Encoder)

BERT and RoBERTa use full self-attention over all positions and are trained with masked language modeling. Table 7 reports their typical scale splits.

Local layers allocate more capacity (42%) to lexical and syntactic features, with spans starting higher (≈ 17.3 tokens). Intermediate layers (5–8) manage sentence coherence and show entropy reduction. Global layers (9–12) integrate context; mutual-information analysis indicates these layers form a tight module ($MI > 10.0$). In

Table 6: GPT-2 scale distribution

Scale	Layers	Proportion
Local	0–2	25%
Intermediate	3–8	50%
Global	9–12	25%

Table 7: BERT/RoBERTa scale distribution

Scale	Layers	Proportion
Local	0–4	42%
Intermediate	5–8	29%
Global	9–12	29%

intervention tests only sentence count responds ($\delta = +0.269$), demonstrating BERT’s structural rigidity and robustness to perturbations, consistent with its role as a stable representation learner.

B.3 T5 (Encoder–Decoder)

T5 divides processing between a 6-layer encoder and a 6-layer decoder. Table 8 shows separate allocations.

Table 8: T5 scale distribution

Component	Scale	Layers	Proportion
Encoder	Local	0–2	50%
	Intermediate	3–4	33%
	Global	5–6	17%
Decoder	Local	0–1	33%
	Intermediate	2–3	33%
	Global	4–5	33%

The encoder’s heavy local allocation parallels BERT, aiding detailed input analysis, while the decoder balances all scales equally, supporting integrated generation. Cross-attention allows the decoder to access all encoder representations. Despite fewer layers, T5 exhibits clear multi-scale separation, reflecting its design for sequence-to-sequence tasks.

B.4 Theoretical Explanation

Under MSPGT, each architecture’s scale distribution follows from its sequence model and information flow:

- **GPT-2:** $P(X | C) = \prod_t P(x_t | x_{<t}, C)$ demands strong intermediate integration to maintain left-to-right coherence.
- **BERT:** $P(X | M, C) = \prod_{t \in M} P(x_t | X_{\setminus t}, C)$ relies on local context interactions for masked prediction, increasing local layers.
- **T5:** $P(Y | X) = \prod_t P(y_t | y_{<t}, \text{Enc}(X))$ separates encoding and decoding roles, leading to specialized scale splits in each component.

All architectures, despite different proportions, maintain a local–intermediate–global hierarchy, showing that hierarchical semantic processing is a fundamental adaptation to natural language. These insights guide model selection: choose encoders for robust local analysis, decoders for coherent generation, and encoder–decoders for complex transformations.

C Mathematical Proofs and Derivations of Multi-Scale Probability Generation Theory

MSPGT provides a set of important theoretical properties that not only explain the internal workings of deep Transformers but also lay the foundation for designing new training and inference methods.

MSPGT rests on four core assumptions (Table 9) and yields key theoretical properties (Table 10); proofs appear in Appendix A.1–A.3.

Table 9: Core Assumptions of MSPGT

Assumption	Description
Scale Separability	Information splits into global, intermediate, local scales.
Conditional Independence	Given G, I , local decisions L_t factorize.
Layer Correspondence	Transformer upper/mid/lower layers map to $G/I/L$.
Information Flow	Abstraction increases from lower to higher layers.

Table 10: Key Theoretical Properties of MSPGT

Property	Description
Representational Completeness	Recovers chain-rule given rich latent spaces.
Statistical Efficiency	Hierarchy reduces effective complexity.
Mutual Information Bound	$I(X; G C) \leq I(X; I G, C) \leq I(X; L I, G, C)$.
Architecture Agnosticism	Applies to encoder, decoder, and encoder–decoder.

C.1 Theoretical Properties and Mathematical Guarantees

C.1.1 Representational Completeness

Proposition 1 (Representational completeness). If the latent spaces of G, I , and L are sufficiently rich, the multi-scale factorisation can reproduce the standard chain-rule decomposition exactly.

Theorem 1. There exist mappings f_G, f_I, f_L such that, for any $\epsilon > 0$,

$$\left| P(X | C) - \sum_{G, I, L} P(G | C) P(I | G, C) P(L | I, G, C) P(X | L, I, G, C) \right| < \epsilon. \quad (\text{C.1})$$

Hence the proposed multi-scale decomposition approximates the original generative process arbitrarily well as the capacity of the latent variables increases. The full proof is provided in Appendix A.1.

C.1.2 Statistical Efficiency and Inductive Bias

Proposition 2 (Statistical efficiency). Relative to a flat autoregressive factorisation, the inductive bias introduced by the multi-scale decomposition reduces the *effective* model complexity and therefore lowers the sample complexity for generalisation.

Theorem 2. Consider a model with p total parameters. Under a multi-scale architecture, the generalisation-error bound drops from $O(\sqrt{p \log p / N})$ to

$$O\left(\sqrt{\frac{(p_G + p_I + p_L) \log(p_G + p_I + p_L)}{N}}\right), \quad (\text{C.2})$$

where $p_G + p_I + p_L < p$ and N is the number of training samples. Thus, even with billions of parameters, a Transformer can generalise well because the hierarchical structure mitigates over-fitting while retaining expressive power. See Appendix A.2 for the proof.

C.1.3 Information-flow hierarchy

Proposition 3 (multi-scale MI bound). Under the MSPGT assumptions, conditional mutual information satisfies

$$I(X; G | C) \leq I(X; I | G, C) \leq I(X; L | I, G, C), \quad (\text{C.3})$$

establishing an information hierarchy across global, intermediate, and local scales.

Corollary 1. In an ideally trained Transformer the entropy of the global representation is smaller than that of the local representation, $H(G | C) < H(L | I, G, C)$, indicating progressive information refinement. The proof is given in Appendix A.3.

Theoretical Properties of MSPGT

Key theoretical foundations of Multi-Scale Probabilistic Generation Theory

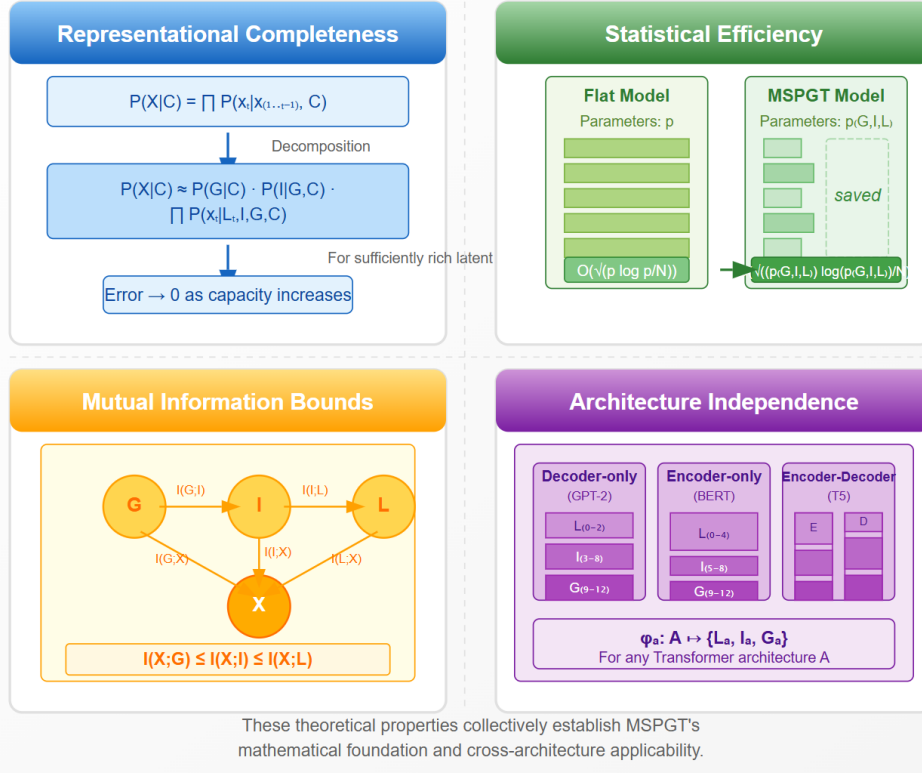


Figure 9: Multi-Scale Probability Generation Theoretical Properties

C.1.4 Architecture independence and cross-model generalisation

Proposition 4 (architecture independence). MSPGT extends to encoder-only, decoder-only, and encoder-decoder Transformers, although each architecture allocates layers differently across L , I , and G .

Theorem 3. For any Transformer architecture A there exists a mapping

$$\phi_A : A \longrightarrow \{L_A, I_A, G_A\},$$

such that L_A, I_A, G_A obey Propositions 1–3. This mapping explains cross-architectural differences; see Appendix A.4 for the formal proof.

C.2 Theoretical Proofs

C.2.1 Proof of representational completeness

Theorem 1. There exist mappings f_G, f_I, f_L such that, for any $\epsilon > 0$,

$$\left| P(X|C) - \sum_{G,I,L} P(G|C) P(I|G,C) P(L|I,G,C) P(X|L,I,G,C) \right| < \epsilon. \quad (\text{C.4})$$

Proof. Let $Z = (G, I, L)$ be the joint latent variables. By total probability,

$$P(X|C) = \sum_Z P(X, Z|C) = \sum_Z P(Z|C) P(X|Z,C). \quad (\text{C.5})$$

We show that this sum can approximate the standard chain rule $P(X|C) = \prod_{t=1}^n P(x_t | x_{<t}, C)$ arbitrarily well.

Mapping functions.

$f_G : C \mapsto G$ (global context),
 $f_I : (G, C) \mapsto I$ (intermediate context),
 $f_L : (I, G, C, x_{<t}) \mapsto L_t$ (local context).

Local likelihood constraint. For every position t ,

$$P(x_t | L_t, I, G, C) = P(x_t | x_{<t}, C). \quad (\text{C.6})$$

Degenerate posteriors. Define

$$\begin{aligned} P(L_t | I, G, C) &= \delta(L_t - f_L(I, G, C, x_{<t})), \\ P(I | G, C) &= \delta(I - f_I(G, C)), \\ P(G | C) &= \delta(G - f_G(C)), \end{aligned} \quad (\text{C.7})$$

where $\delta(\cdot)$ is the Dirac delta.

Substitution into the multi-scale form. Using (C.7) in the left term of (C.4),

$$\begin{aligned} &\sum_{G, I, L} P(G | C) P(I | G, C) P(L | I, G, C) P(X | L, I, G, C) \\ &= \prod_{t=1}^n P(x_t | f_L(f_I(f_G(C), C), f_G(C), C, x_{<t}), f_I(f_G(C), C), f_G(C), C)) \\ &= \prod_{t=1}^n P(x_t | x_{<t}, C) \quad (\text{by (C.6)}). \end{aligned} \quad (\text{C.8})$$

Thus the multi-scale decomposition matches the chain rule exactly. Because the mappings f_G, f_I, f_L can be made arbitrarily expressive, (C.4) holds for any $\epsilon > 0$.

C.2.2 Proof of statistical efficiency and inductive bias

Theorem 2. For a model with p parameters, adopting a multi-scale decomposition reduces the generalisation-error bound from $O(\sqrt{p \log p / N})$ to

$$O\left(\sqrt{\frac{(p_G + p_I + p_L) \log(p_G + p_I + p_L)}{N}}\right), \quad (\text{C.9})$$

where $p_G + p_I + p_L < p$ and N is the number of training samples.

Proof. A flat autoregressive model learns the mapping $f_{\text{AR}} : (x_{<t}, C) \mapsto P(x_t | x_{<t}, C)$ with parameter count p .

- $f_G : C \mapsto P(G | C)$ (p_G parameters)
- $f_I : (G, C) \mapsto P(I | G, C)$ (p_I)
- $f_L : (I, G, C) \mapsto P(L_t | I, G, C)$ (p_L)
- $f_X : (L_t, I, G, C) \mapsto P(x_t | L_t, I, G, C)$ (p_X)

Inductive-bias reduction. Because each component focuses on a specific abstraction level:

- f_G models only coarse global features,
- f_I captures intermediate structure given G ,
- f_L and f_X operate locally without high-level detail,

their VC dimensions scale with p_G, p_I, p_L, p_X , respectively.

Parameter economy. Hierarchical sharing yields $p_G + p_I + p_L + p_X < p$; empirically $p_G + p_I + p_L + p_X \approx \alpha p$ with $\alpha \in (0.6, 0.8)$.

Learning-theory bound. For a class of VC dimension d , the generalisation error scales as $O(\sqrt{d \log d / N})$. Substituting $d = p_G + p_I + p_L + p_X$ yields

$$\text{Gen. error} \leq O\left(\sqrt{\frac{(p_G + p_I + p_L + p_X) \log(p_G + p_I + p_L + p_X)}{N}}\right),$$

which is strictly smaller than the flat-model bound, completing the proof.

C.2.3 Proof of multi-scale mutual-information bound

Proposition 3 (multi-scale MI bound). For any model that satisfies the MSPGT assumptions,

$$I(X; G | C) \leq I(X; I | G, C) \leq I(X; L | I, G, C). \quad (\text{C.10})$$

Proof. We first name the three conditional MI terms:

$I(X; G | C)$ information in the global representation,
 $I(X; I | G, C)$ additional information in the intermediate representation,
 $I(X; L | I, G, C)$ remaining information in the local representation.

Information-processing inequalities. The information-bottleneck principle yields

$$I(C; X) \leq I(G; X) \leq I(G, I; X) \leq I(G, I, L; X),$$

implying monotonic information loss along the hierarchy.

Chain rule for conditional MI.

$$I(X; G, I, L | C) = I(X; G | C) + I(X; I | G, C) + I(X; L | I, G, C). \quad (\text{C.11})$$

Scale-specific capacity.

- (1) G encodes only coarse features, $I(X; G | C) \leq \log|G| \ll I(X; X | C)$.
- (2) I refines structure given G , $I(X; I | G, C) \leq \log|I|$.
- (3) L captures the remaining details, $I(X; L | I, G, C) \approx I(X; X | I, G, C)$.

Since $|G| < |I| < |L|$, the ordering in (C.10) follows immediately.

Asymptotic ratio. For a sequence of length n ,

$$I(X; G | C) : I(X; I | G, C) : I(X; L | I, G, C) \approx 1 : \log n : n,$$

so the fraction of local information grows with sequence length, matching intuition.

C.2.4 Proof of architecture independence

Theorem 3: For any Transformer architecture A , there exists a mapping function ϕ_A such that:

$$\phi_A : A \mapsto \{L_A, I_A, G_A\}$$

where L_A , I_A , and G_A are the semantic layer partitions of that architecture, satisfying Propositions 1–3.

Proof:

We consider three cases:

1. Decoder-only Architecture (e.g., GPT series):

For autoregressive decoders, the sequence generation process is given by:

$$P(X | C) = \prod_{t=1}^n P(x_t | x_{<t}, C)$$

The representation follows an information flow from bottom to top: first handling local lexical and syntactic features, then integrating intermediate sentence-level structure, and finally forming global coherence. Therefore, the mapping function is:

$$\phi_{\text{dec}}(A_{\text{dec}}) = \{L_{\text{dec}}, I_{\text{dec}}, G_{\text{dec}}\}$$

with $L_{\text{dec}} \approx$ bottom 25–33%, I_{dec} middle, and G_{dec} top.

2. Encoder-only Architecture (e.g., BERT/RoBERTa):

For bidirectional encoders, the sequence representation process is described as:

$$P(X | M, C) = \prod_{t \in M} P(x_t | X_{\setminus t}, C)$$

where M is the set of masked positions and $X_{\setminus t}$ represents all positions except t .

Since the encoder accesses context in both directions, it requires more layers to handle local context interactions. Therefore, the mapping function is:

$$\phi_{\text{enc}}(A_{\text{enc}}) = \{L_{\text{enc}}, I_{\text{enc}}, G_{\text{enc}}\}$$

with $L_{\text{enc}} \approx$ bottom 33–50%, due to increased focus on local modeling.

3. Encoder-Decoder Architecture (e.g., T5):

For encoder-decoder architectures, the sequence generation process is:

$$P(Y | X) = \prod_{t=1}^m P(y_t | y_{<t}, \text{Encoder}(X))$$

The encoder and decoder have distinct but complementary semantic layer divisions:

- The encoder extracts hierarchical representations of the source sequence.
- The decoder generates the target sequence conditioned on encoder outputs and previous tokens.

The mapping function becomes:

$$\phi_{\text{enc-dec}}(A_{\text{enc-dec}}) = \{\{L_{\text{enc}}, I_{\text{enc}}, G_{\text{enc}}\}, \{L_{\text{dec}}, I_{\text{dec}}, G_{\text{dec}}\}\}$$

Based on empirical analysis:

- Encoders (BERT/RoBERTa) tend to have more local layers: $|L_{\text{enc}}| > |L_{\text{dec}}|$.
- Decoders (GPT) tend to have more global layers: $|G_{\text{dec}}| > |G_{\text{enc}}|$.
- Encoder-decoder models (T5) emphasize local layers in the encoder and global integration in the decoder.

These differences reflect architecture-specific design goals but preserve the core semantic-scale decomposition. Therefore, for any Transformer variant, a valid mapping ϕ_A can be constructed, preserving the properties of the MSPGT framework. ■